Inorg. Chem. **2006**, *45*, 10678–10687

Synthesis, Spectroscopic, and Structural Investigation of the Cyclic $[N(PR_2E)_2]^+$ Cations (E = Se, Te; R = ^{i}Pr, Ph): the Effect of Anion and R-Group Exchange

Jari Konu,[†] Tristram Chivers,*[,†] and Heikki M. Tuononen[‡]

Department of Chemistry, University of Calgary, 2500 University Drive Northwest, Calgary, Alberta, Canada T2N 1N4, and Department of Chemistry, University of Jyväskylä, P.O. Box 35, Jyväskylä, FI-40014, Finland

Received August 15, 2006

Two-electron oxidation of the $[N(P^iPr_2E)_2]^-$ anion with iodine produces the cyclic $[N(P^iPr_2E)_2]^+$ (E = Se, Te) cations, which exhibit long E–E bonds in the iodide salts $[N(P^iPr_2Se)_2]I$ (**4**) and $[N(P^iPr_2Te)_2]I$ (**5**). The iodide salts **4** and **5** are converted to the ion-separated salts $[N(P^iPr_2Se)_2]SbF_6$ (**6**) and $[N(P^iPr_2Te)_2]SbF_6$ (**7**) upon treatment with $AgSbF_6$. Compounds **4**–**7** were characterized in solution by multinuclear NMR, vibrational, and UV–visible spectroscopy supported by DFT calculations. A structural comparison of salts **4**–**7** and $[N(P^iPr_2Te)_2]Cl$ (**8**) confirms that the long E–E bonds in **4**, **5**, and **8** can be attributed primarily to the donation of electron density from a lone pair of the halide counterion into the E–E σ^* orbital (LUMO) of the cation. The phenyl derivative $[N(PPh_2Te)_2]I$ (**9**) was prepared in a similar manner. However, the attempted synthesis of the selenium analogue, $[N(PPh_2Se)_2]I$, produced a 1:1 mixture of $[N(PPh_2Se)_2(\mu\text{-Se})][I]$ (**10**) and $[SeP(Ph_2)N(Ph_2)PI]$ (**11**). DFT calculations of the formation energies of **10** and **11** support the observed decomposition. Compound **10** is a centrosymmetric dimer in which two six-membered NP_2Se_3 rings are bridged by two I^- anions. Compound **11** produces the nine-atom chain $\{[N(PPh_2)_2\text{-}Se]_2(\mu\text{-O})\}$ (**12**) upon hydrolysis during crystallization. The reaction between $[(TMEDA)NaN(P^iPr_2Se)_2]$ and $SeCl_2$ in a 1:1 molar ratio yields the related acyclic species $[SeP(^iPr_2)N(^iPr_2)PCl]$ (**13**), which was characterized by multinuclear NMR spectroscopy and an X-ray structural determination.

Introduction

Dichalcogenoimidodiphosphinate ligands $[N(PR_2E)_2]^-$ **1** (E = O, S, Se) have a long and venerable history that dates back to the 1960s.[1] The widespread interest in their metal complexes[2] arises from a number of potential uses, e.g., as lanthanide shift reagents,[3] in luminescent materials,[4] or in metal extraction processes.[5] Recently, O'Brien and co-workers have demonstrated that certain complexes of the isopropyl derivatives **1a** and **1b** are sufficiently volatile to

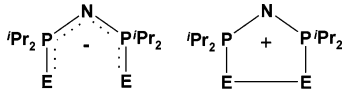

1a (E = S)
1b (E = Se)
1c (E = Te)

3a (E = S)
3b (E = Se)
3c (E = Te)

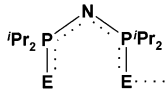

2a (E = S)
2b (E = Se)
2c (E = Te)

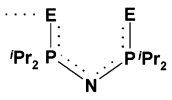

serve as single-source precursors for the production of thin semiconducting films of metal selenides.[6]

The neutral precursors to the anionic ligands **1a** and **1b** are readily made by direct reaction of $HN(P^iPr_2)_2$ with

* To whom correspondence should be addressed. E-mail: chivers@ucalgary.ca. Tel: +1-403-220-5741. Fax: +1-403-289-9488.
[†] University of Calgary.
[‡] University of Jyväskylä.

(1) (a) Schmidpeter, A.; Bohm, R.; Groeger, H. *Angew. Chem., Int. Ed. Engl.* **1964**, *3*, 704. (b) Schmidpeter, A.; Stoll, K. *Angew. Chem., Int. Ed. Engl.* **1967**, *6*, 252. (c) Schmidpeter, A.; Stoll, A. *Angew. Chem., Int. Ed. Engl.* **1968**, *7*, 549.
(2) For reviews of early work, see (a) Silvestru, C.; Drake, J. E. *Coord. Chem. Rev.* **2001**, *223*, 117. (b) Ly, T. Q.; Woollins, J. D. *Coord. Chem. Rev.* **1998**, *176*, 451. (c) Haiduc, I. In *Comprehensive Coordination Chemistry II*; McCleverty, J. A., Meyer, T. J., Eds.; Elsevier Ltd: Amsterdam, 2003; pp 323−347.
(3) Rudler; H.; Denise, B.; Gregorio, J. R.; Vaissermann, J. *Chem. Commun.* **1997**, 229.
(4) Magennis, S. W.; Parsons, S.; Corval, A.; Woollins, J. D.; Pikramenou, Z. *Chem. Commun.* **1999**, 61.

10.1021/ic061545i CCC: $33.50
Published on Web 11/04/2006

elemental sulfur or selenium, respectively,[7] but this reaction is not successful for the synthesis of $HN(P^iPr_2Te)_2$. Four years ago, we reported the synthesis of the tellurium-containing ligands $[N(PR_2Te)_2]^-$ (R = ^{i}Pr, Ph) by metalation of $HN(PR_2)_2$ with NaH *prior to reaction with tellurium*.[8,9] The discovery of this new synthetic approach has opened the door to a wide-ranging study of metal complexes of **1c**. To date, homoleptic complexes of Group 12 (Zn, Cd, Hg) and Group 15 (Sb, Bi),[10] as well as a La(III) complex and the first example of a covalent actinide−tellurium bond, have been reported.[11] Some of these complexes have been shown to be suitable single-source precursors for metal telluride thin films or nanoparticles, e.g., CdTe,[12] Sb_2Te_3.[13] In contrast to the metathetical reactions observed for Groups 12 and 15 halides, the treatment of **1c** with Group 13 (Ga, In) trihalides gives rise to a novel tellurium-transfer process and the formation of Ga_2Te_2 and In_3Te_3 rings.[14]

An intriguing feature of the chemistry of **1c** is the formation of unusual dichalcogenides of the type **2** upon one-electron oxidation of the sodium salts with iodine.[9,15] This redox process represents a new aspect of the well-studied chemistry of dichalcogenoimidodiphosphinates and raised the fascinating question of whether the corresponding cations **3b** and **3c** can be prepared by two-electron oxidation of the corresponding anions **1b** or **1c** (or one-electron oxidation of the dimers **2b** and **2c**). In a preliminary communication,[16] we described the synthesis of the iodide salts $[N(P^iPr_2Se)_2]I$ (**4**) and $[N(P^iPr_2Te)_2]I$ (**5**), which contain the cyclic cations **3b** and **3c**, respectively. Simple electron-counting procedures for these novel inorganic heterocycles predict a six π-electron system.[17] However, DFT calculations revealed that, although the three highest occupied molecular orbitals in the five-membered rings **3** are π-type orbitals, the bonding effect of the E−E π-bonding orbital (HOMO-2) is essentially canceled by the double occupation of the E−E π*-antibonding orbital (HOMO). Since the third π orbital (HOMO-1) is a non-bonding orbital located primarily on the nitrogen atom, the π-bond order of the ring system is approximately zero.

DFT calculations also indicated that the unusually long chalcogen−chalcogen bonds observed in the iodide salts **4** and **5** may be attributed primarily to donation of electron density from a lone pair of the iodide counterion into the E−E σ* orbital (LUMO) of the cyclic cation.[16] We have now extended the investigation of this new five-membered ring system to include ion-separated salts in order to gain experimental verification for this explanation. In addition, the effect of the replacement of the isopropyl substituents on phosphorus by phenyl groups was examined. Thus, we report herein the synthesis, spectroscopic and structural characterization of the following salts of these five-membered rings $[N(P^iPr_2Se)_2]SbF_6$ (**6**), $[N(P^iPr_2Te)_2]SbF_6$ (**7**), $[N(P^iPr_2Te)_2]Cl$ (**8**), and $[N(PPh_2Te)_2]I$ (**9**). The unexpected formation of the six-membered ring $[N(PPh_2Se)_2(\mu\text{-Se})][I]$ (**10**) and the acyclic species $[SeP(Ph_2)N(Ph_2)PI]$ (**11**) in the attempted synthesis of $[N(PPh_2Se)_2]I$ is also described together with the X-ray structure of the nine-atom chain $\{[N(PPh_2)_2Se]_2(\mu\text{-O})\}\cdot CH_2Cl_2$ (**12**$\cdot CH_2Cl_2$). The synthesis and X-ray structure of the acyclic compound $[SeP(^iPr_2)N(^iPr_2)PCl]$ (**13**), an analogue of **11**, are also discussed.

Experimental Section

General Procedures. All reactions and manipulations of products were performed under an argon atmosphere by using standard Schlenk techniques or an inert atmosphere glovebox. $[N(P^iPr_2E)_2]I$ (**4**, E = Se; **5**, E = Te) were prepared by the method described recently.[16] The complete spectroscopic data (^{1}H, ^{13}C, ^{31}P, ^{77}Se, ^{125}Te NMR, IR and Raman, UV−visible) and relevant bond parameters for **4** and **5** are included here for comparison with those of **6** and **7**. The reagents $[(TMEDA)NaN(PR_2E)_2]$ (E = Se, Te; R = ^{i}Pr, Ph) were prepared by modifications of the procedure reported for $[(TMEDA)NaN(PPh_2Te)_2]$.[8] $SeCl_2$ was prepared from red selenium and SO_2Cl_2 in THF.[18] The solvents *n*-hexane, toluene, and THF were dried by distillation over Na/benzophenone and CH_2Cl_2 over P_2O_5 under a nitrogen atmosphere prior to use.

Spectroscopic Methods. The ^{1}H, ^{13}C, ^{31}P, ^{77}Se, and ^{125}Te NMR spectra were obtained in d_8-THF or CD_2Cl_2 on a Bruker DRX 400 spectrometer operating at 399.592, 100.489, 161.765, 76.223, and 126.082 MHz, respectively. ^{1}H and ^{13}C spectra are referenced to the solvent signal, and the chemical shifts are reported relative to $(CH_3)_4Si$. ^{31}P and ^{77}Se NMR spectra are referenced externally to an 85% solution of H_3PO_4 and to a saturated solution of SeO_2 in D_2O, respectively, and the chemical shifts are reported relative to H_3PO_4 and to neat Me_2Se [$\delta(Me_2Se) = \delta(SeO_2) + 1302.6$]. The ^{125}Te NMR spectra are referenced externally to a saturated solution of H_6TeO_6 and the ^{125}Te chemical shifts are reported relative to Me_2Te [$\delta(Me_2Te) = \delta(H_6TeO_6) + 712$].

Raman spectra were recorded at the University of Lethbridge from solid samples at −100 °C by using a Bruker RFS 100 FT-Raman spectrometer with a quartz beam splitter, liquid-nitrogen-cooled Ge detector and Nd:YAG laser (power 25−100 mW; 500−1000 scans; spectral resolution ±2 to ±8 cm^{-1}; Blackmann−Harris four-term apodization; scattering geometry 180 °). IR spectra were measured as Nujol mulls between KBr plates on a Mattson Genesis Series FT-IR (4000−400 cm^{-1}) spectrometer. A list of IR and

(5) du Preez, J. G. H.; Knabl, K. U.; Krüger, L.; van Brecht, B. J. A. M. *Solvent Extr. Ion Exch.* **1992**, *10*, 729.
(6) For selected examples, see (a) Afzall, M.; Crouch, D.; Malik, M. A.; Motevalli, M.; O'Brien, P.; Park, J.-H.; Woollins, J. D. *Eur. J. Inorg. Chem.* **2004**, 171. (b) Afzall, M.; Ellwood, K.; Pickett, N. L.; O'Brien, P.; Raftery, J.; Waters, J. *J. Mater. Chem.* **2004**, *14*, 1310. (c) Waters, J.; Crouch, D.; Raftery, J.; O'Brien, P. *Chem. Mater.* **2004**, *16*, 3289.
(7) Cupertino, D.; Birdsall, D. J.; Slawin, A. M. Z.; Woollins, J. D. *Inorg. Chim. Acta* **1999**, *290*, 1.
(8) Briand, G. G.; Chivers, T.; Parvez, M. *Angew. Chem., Int. Ed.* **2002**, *41*, 3468.
(9) Chivers, T.; Eisler, D. J.; Ritch, J. S.; Tuononen, H. M. *Angew. Chem., Int. Ed.* **2005**, *44*, 4953.
(10) Chivers, T.; Eisler, D. J.; Ritch, J. S. *Dalton Trans.* **2005**, 2675.
(11) Gaunt, A. J.; Scott, B. L.; Neu, M. P. *Angew. Chem., Int. Ed.* **2006**, *45*, 1638.
(12) Garje, S. S.; Ritch, J. S.; Eisler, D. J.; Afzaal, M.; O'Brien, P.; Chivers, T. *J. Mater. Chem.* **2006**, 966.
(13) Garje, S. S.; Eisler, D. J.; Ritch, J. S.; Afzaal, M.; O'Brien, P.; Chivers, T. *J. Am. Chem. Soc.* **2006**, *128*, 3120.
(14) Copsey, M. C.; Chivers, T. *Chem. Commun.* **2005**, 4938.
(15) The sulfur analogue **2a** (R = ^{t}Bu derivative) and the selenium analogues **2b** (R = ^{i}Pr, ^{t}Bu derivatives) have been prepared in a similar manner and shown to have dimeric structures with elongated E−E bonds: Chivers, T.; Eisler, D. J.; Ritch, J. S. Manuscript in preparation.
(16) Konu, J.; Chivers, T.; Tuononen, H. M. *Chem. Commun.* **2006**, 1634.
(17) Chivers, T. *A Guide to Chalcogen-Nitrogen Chemistry*; World Scientific: Singapore, 2005; Chapter 4, pp 60−63.
(18) Maaninen, A.; Chivers, T.; Parvez, M.; Pietikäinen, J.; Laitinen, R. S. *Inorg. Chem.* **1999**, *38*, 4093.

Raman vibrations can be found in the Supporting Information (Table S1). Elemental analyses were performed by Analytical Services, Department of Chemistry, University of Calgary. UV−visible spectra were measured with a Cary 50 spectrophotometer (200−800 nm, scan rate 600 nm/min, dual beam) in CH_2Cl_2 and MeCN.

Spectroscopic data of [N(P^{i}Pr$_2$Se)$_2$]I (4).[16] ^{1}H NMR (d_8-THF, 23 °C): δ 2.73 [2 × sept, $^3J(^1H,^1H) = 7$ Hz, 4H; C*H*(CH$_3$)$_2$], 1.37 [dd, $^3J(^1H,^1H) = 7$ Hz, $^3J(^1H,^{31}P) = 18$ Hz, 12H; CH(C*H*$_3$)$_2$], 1.35 [dd, $^3J(^1H,^1H) = 7$ Hz, $^3J(^1H,^{31}P) = 20$ Hz, 12H; CH(C*H*$_3$)$_2$]; ^{13}C{^{1}H} NMR: δ 33.2 (m, 4C; *C*H(CH$_3$)$_2$), 18.6 (s, 4C; CH(*C*H$_3$)$_2$), 17.7 (s, 4C; CH(*C*H$_3$)$_2$); ^{31}P{^{1}H} NMR: δ 92.8 [s, $^1J(^{77}Se,^{31}P) = 440$ Hz, $^2J(^{31}P,^{31}P) = 34$ Hz];^{77}Se NMR: δ 297 (br, d, $^1J(^{77}Se,^{31}P) = 430$ Hz). UV−vis (CH_2Cl_2): 230−270 and 365 nm (ϵ 1.7 × 10^4 mol^{-1} cm^{-1}).

Spectroscopic data of [N(P^{i}Pr$_2$Te)$_2$]I (5).[16] ^{1}H NMR (d_8-THF, 23 °C): δ 2.62 [2 × sept, $^3J(^1H,^1H) = 7$ Hz, 4H; C*H*(CH$_3$)$_2$], 1.35 [dd, $^3J(^1H,^1H) = 7$ Hz, $^3J(^1H,^{31}P) = 18$ Hz, 12H; CH(C*H*$_3$)$_2$], 1.31 [dd, $^3J(^1H,^1H) = 7$ Hz, $^3J(^1H,^{31}P) = 20$ Hz, 12H; CH(C*H*$_3$)$_2$]; ^{13}C{^{1}H} NMR: δ 33.1 (m, 4C; *C*H(CH$_3$)$_2$), 19.6 (s, 4C; CH(*C*H$_3$)$_2$), 18.1 (br, s, 4C; CH(*C*H$_3$)$_2$); ^{31}P{^{1}H} NMR: δ 68.1 [s, $^1J(^{125}Te,^{31}P) = 1040$ Hz, $^2J(^{31}P,^{31}P) = 31$ Hz]. UV−vis (CH_2Cl_2): 230−270 and 365 nm ($\epsilon = 3.7 \times 10^4$ mol^{-1} cm^{-1}).

Synthesis of [N(P^{i}Pr$_2$Se)$_2$]SbF$_6$ (6). A solution of **4** (0.213 g, 0.40 mmol) in 25 mL of toluene was cooled to −80 °C, and a solution of $AgSbF_6$ (0.137 g, 0.40 mmol) in 25 mL of toluene was added slowly via cannula. The reaction mixture was stirred for 1 h at −80 °C and 2 h at 23 °C. Solvent was evaporated under vacuum, and the resulting orange precipitate was dissolved to ca. 50 mL of THF. AgI was allowed to settle, and the solution was filtered through a microfilter (0.45 μm PTFE) and then dried under vacuum yielding an orange, slightly sticky powder (0.200 g, 78%). Elemental analysis calcd (%) for $C_{12}H_{28}F_6N_1P_2Sb_1Se_2$: C 22.45, H 4.40, N 2.18; found: C 23.21, H 4.47, N 2.31. ^{1}H NMR (d_8-THF, 23 °C): δ 2.82 [2 × sept, $^3J(^1H,^1H) = 7$ Hz, 4H; C*H*(CH$_3$)$_2$], 1.42 [dd, $^3J(^1H,^1H) = 7$ Hz, $^3J(^1H,^{31}P) = 20$ Hz, 12H; CH(C*H*$_3$)$_2$], 1.40 [dd, $^3J(^1H,^1H) = 7$ Hz, $^3J(^1H,^{31}P) = 21$ Hz, 12H; CH(C*H*$_3$)$_2$]; ^{13}C{^{1}H} NMR: δ 31.4 (m, 4C; *C*H(CH$_3$)$_2$), 17.7 [s, 4C; CH(*C*H$_3$)$_2$], 17.4 [s, 4C; CH(*C*H$_3$)$_2$]; ^{31}P{^{1}H} NMR: δ 113.2 [s, $^1J(^{77}Se,^{31}P) = 363$ Hz, $^2J(^{31}P,^{31}P) = 45$ Hz]; ^{77}Se NMR: δ 344 [d, $^1J(^{77}Se,^{31}P) = 360$ Hz]. UV−vis (CH_2Cl_2): λ 230−270 and 365 nm ($\epsilon = 1.1 \times 10^3$ mol^{-1} cm^{-1}). X-ray-quality crystals were obtained by layering toluene on top of a THF solution of **6**.

Synthesis of [N(P^{i}Pr$_2$Te)$_2$]SbF$_6$ (7). The salt **7** was obtained as a dark blue, slightly sticky powder (0.235 g, 80%) from the reaction of **5** (0.252 g, 0.40 mmol) in 25 mL of toluene with $AgSbF_6$ (0.137 g, 0.40 mmol) in 25 mL of toluene by using a procedure identical to that described above for **6**. Elemental analysis calcd (%) for $C_{12}H_{28}F_6N_1P_2Sb_1Te_2$: C 19.50, H 3.82, N 1.89; found: C 20.16, H 3.86, N 2.01. ^{1}H NMR (d_8-THF, 23 °C): δ 2.64 [2 × sept, $^3J(^1H,^1H) = 7$ Hz, 4H; C*H*(CH$_3$)$_2$], 1.37 [dd, $^3J(^1H,^1H) = 7$ Hz, $^3J(^1H,^{31}P) = 19$ Hz, 12H; CH(C*H*$_3$)$_2$], 1.34 [dd, $^3J(^1H,^1H) = 7$ Hz, $^3J(^1H,^{31}P) = 21$ Hz, 12H; CH(C*H*$_3$)$_2$]; ^{13}C{^{1}H} NMR: δ 32.3 (m, 4C; *C*H(CH$_3$)$_2$), 19.1 [s, 4C; CH(*C*H$_3$)$_2$], 18.0 [s, 4C; CH(*C*H$_3$)$_2$]; ^{31}P{^{1}H} NMR: δ 85.7 [s, $^1J(^{125}Te,^{31}P) = 863$ Hz, $^2J(^{31}P,^{31}P) = 39$ Hz]; ^{125}Te NMR: δ 254 [d, $^1J(^{125}Te,^{31}P) = 870$ Hz]. UV−vis: λ 230−270, 365 ($\epsilon = 3.6 \times 10^3$ mol^{-1} cm^{-1}), and 595 nm ($\epsilon = 190$ mol^{-1} cm^{-1}) in CH_2Cl_2; λ 230−270, 365 ($\epsilon = 3.2 \times 10^3$ mol^{-1} cm^{-1}), and 560 nm ($\epsilon = 200$ mol^{-1} cm^{-1}) in MeCN. X-ray-quality crystals were grown by layering *n*-hexane on top of a THF solution of **7**.

Formation of [N(P^{i}Pr$_2$Te)$_2$]Cl (8). A few X-ray-quality crystals of **8** were obtained from the reaction solution of an equimolar reaction between [N(P^{i}Pr$_2$Te)$_2$]$_2$ and SO_2Cl_2 in toluene. The reaction yielded a complex mixture of products, as shown by the ^{31}P NMR spectroscopy, and therefore, the compound **8** was not obtained as pure product in reasonable yield.

Synthesis of [N(PPh$_2$Te)$_2$]I (9). A solution of [(TMEDA)NaN(PPh$_2$Te)$_2$] (0.389 g, 0.50 mmol) in 35 mL of toluene was cooled to −80 °C, and a solution of I_2 (0.127 g, 0.50 mmol) in 15 mL of THF was added slowly via cannula. The resulting red solution was stirred for 1 h at −80 °C and 2 h at 23 °C. A dark red precipitate was allowed settle, and the orange solution was decanted via cannula. The precipitate was dried under vacuum and then washed with MeCN affording **9** as red-brown powder (0.253 g, 66%). Elemental analysis calcd (%) for $C_{24}H_{20}I_1N_1P_2Te_2$: C 37.61, H 2.63, N 1.83; found: C 36.91, H 2.45, N 1.75. ^{1}H NMR (CD_2Cl_2, 23 °C): δ 7.76 (m), 7.57 (m), 7.46 (m); ^{31}P{^{1}H} NMR: δ 21.9 [s, $^1J(^{125}Te,^{31}P) = 1066$ Hz]. X-ray-quality crystals of **9** were grown from CH_2Cl_2.

Reaction of [(TMEDA)NaN(PPh$_2$Se)$_2$] with I$_2$. A slurry of [(TMEDA)NaN(PPh$_2$Se)$_2$] (0.273 g, 0.40 mmol) in 35 mL of *n*-hexane was cooled to −80 °C, and a solution of I_2 (0.102 g, 0.40 mmol) in 15 mL of toluene was added slowly via cannula. The resulting red solution was stirred for 1 h at −80 °C and 2 h at 23 °C. The precipitate was allowed settle, and the orange-yellow solution was decanted via cannula. The precipitate was dried under vacuum and then washed with MeCN affording an orange-yellow powder (0.241 g, 90% in *n*-hexane/toluene, calculated as a 1:1 mixture of **10** and **11**). A slightly lower yield was obtained when the reaction was carried out in an *n*-hexane/THF mixture. ^{31}P{^{1}H} NMR (d_8-THF, 23 °C): δ 49.5 [s, br, $^1J(^{31}P,^{77}Se) = 447$ Hz] (**10**), 36.1 [s, $^1J(^{77}Se,^{31}P) = 745$ Hz] (**11**), 24.3 (s) (**11**). X-ray-quality crystals of **10** were grown from CH_2Cl_2. Attempts to grow X-ray-quality crystals of **11** from CH_2Cl_2 produced crystals of the hydrolysis product **12**.

Reaction of [(TMEDA)NaN(P^{i}Pr$_2$Se)$_2$] with SeCl$_2$. A freshly prepared solution of $SeCl_2$ (0.039 g of red selenium and 0.067 g of SO_2Cl_2, 0.50 mmol)[18] in ca. 1 mL of THF was added to a slurry of [(TMEDA)NaN(P^{i}Pr$_2$Se)$_2$] (0.273 g, 0.50 mmol) in ca. 40 mL of *n*-hexane at −80 °C. The reaction mixture was stirred for 1 h at −80 °C and 2 h at 23 °C, resulting in a pale yellow solution and a mixture of red and white powders. The solution was decanted via cannula and, after several days at −20 °C, produced colorless crystals of [SeP(*i*Pr$_2$)N(*i*Pr$_2$)PCl] (**13**) (0.071 g, 39%). The main component of the powders (0.148 g) was shown to be **13** by ^{31}P NMR spectroscopy. Elemental analysis calcd (%) for $C_{14}H_{28}Cl_1N_1P_2Se_1$: C 39.74, H 7.78, N 3.86; found: C 39.94, H 7.90, N 4.51. ^{1}H NMR (D$_8$-THF, 23 °C): δ 2.71 [2 × sept, $^3J(^1H,^1H) = 7.1$ Hz, 4H; C*H*(CH$_3$)$_2$], 2.02 [2 × sept, $^3J(^1H,^1H) = 6.9$ Hz, 4H; C*H*(CH$_3$)$_2$], 1.36 [dddd, $^3J(^1H,^{31}P) = 20.0$ Hz, $^3J(^1H,^1H) = 7.1$ Hz, 6H; CH(C*H*$_3$)$_2$], 1.15 [dd, $^3J(^1H,^{31}P) = 17.1$ Hz, $^3J(^1H,^1H) = 6.9$ Hz, 6H; CH(C*H*$_3$)$_2$]; ^{13}C{^{1}H} NMR: δ 33.0 [m, 2C; *C*H(CH$_3$)$_2$)], 33.2 [m, 2C; *C*H(CH$_3$)$_2$)], 17.6 [s, 2C; CH(*C*H$_3$)$_2$], 17.1 [m, 4C; CH(*C*H$_3$)$_2$], 16.9 [m, 2C; CH(*C*H$_3$)$_2$]; ^{31}P{^{1}H} NMR: δ 67.2 [d, $^1J(^{77}Se,^{31}P) = 722$ Hz, $^2J(^{31}P,^{31}P) = 37$ Hz], 66.0 [d, $^2J(^{31}P,^{31}P) = 37$ Hz];^{77}Se NMR: δ −308 [d, $^1J(^{77}Se,^{31}P) = 722$ Hz].

X-ray Crystallography. Crystals of **6**−**10**, **12**, and **13** were coated with Paratone 8277 oil and mounted on a glass fiber. Diffraction data were collected on a Nonius KappaCCD diffractometer using monochromated Mo K$_\alpha$ radiation ($\lambda = 0.71073$ Å) at −100 °C. The data sets were corrected for Lorentz and polarization effects, and empirical absorption correction was applied to the net intensities. The structures were solved by direct methods using SHELXS-97[19] and refined using SHELXL-97.[20] After the full-matrix least-squares refinement of the non-hydrogen atoms with anisotropic thermal parameters, the hydrogen atoms were placed

Table 1. Crystallographic Data for $[N(P^iPr_2Se)_2]SbF_6$ (**6**), $[N(P^iPr_2Te)_2]SbF_6$ (**7**), $[N(P^iPr_2Te)_2]Cl$ (**8**), $[N(PPh_2Te)_2]I$ (**9**), $[N(PPh_2Se)_2(\mu\text{-Se})][I]$ (**10**), $\{[N(PPh_2)_2Se]_2(\mu\text{-O})\}\cdot CH_2Cl_2$ (**12**·CH_2Cl_2), and $[SeP(^iPr_2)N(^iPr_2)PCl]$ (**13**)[a]

	6	**7**	**8**	**9**	**10**	**12**	**13**
empirical formula	$C_{12}H_{28}F_6NP_2SbSe_2$	$C_{12}H_{28}F_6NP_2SbTe_2$	$C_{12}H_{28}ClNP_2Te_2$	$C_{24}H_{20}INP_2Te_2$	$C_{24}H_{20}INP_2Se_3$	$C_{49}H_{42}Cl_2N_2OP_4Se_2$	$C_{12}H_{28}ClNP_2Se$
fw	641.96	739.24	538.94	766.45	748.13	1027.55	362.70
cryst syst	triclinic	monoclinic	monoclinic	triclinic	monoclinic	monoclinic	orthorhombic
space group	$P\bar{1}$	$P2_1/n$	$P2_1/c$	$P\bar{1}$	$P2_1/c$	$C2/c$	$P2_12_12_1$
a, Å	8.877(2)	9.996(2)	7.398(2)	10.592(2)	9.424(2)	10.765(2)	7.038(1)
b, Å	10.205(2)	8.960(2)	17.778(4)	11.125(2)	20.694(4)	20.093(4)	13.483(3)
c, Å	13.078(3)	25.778(5)	14.918(3)	12.264(3)	13.016(3)	21.546(4)	18.421(4)
α, deg	68.38(3)	90.00	90.00	95.51(3)	90.00	90.00	90.00
β, deg	79.18(3)	90.24(3)	103.27(3)	100.35(3)	95.07(3)	92.34(3)	90.00
γ, deg	88.16(3)	90.00	90.00	117.98(3)	90.00	90.00	90.00
V, Å^3	1080.9(5)	2308.7(8)	1909.6(7)	1228.1(6)	2528.6(9)	4657(2)	1748.0(6)
Z	2	4	4	2	4	4	4
T, °C	−100	−100	−100	−100	−100	−100	−100
ρ_{calcd}, g/cm^3	1.972	2.127	1.875	2.073	1.965	1.466	1.378
μ(Mo Kα), mm^{-1}	4.837	3.854	3.350	3.774	5.725	1.879	2.468
cryst size, mm^3	0.28 × 0.24 × 0.24	0.16 × 0.16 × 0.08	0.36 × 0.16 × 0.16	0.08 × 0.04 × 0.03	0.12 × 0.04 × 0.01	0.12 × 0.08 × 0.08	0.16 × 0.16 × 0.16
F(000)	620	1384	1032	716	1424	2080	752
Θ range, deg	3.71−25.03	3.15−25.03	3.62−25.03	2.25−25.02	2.75−25.01	2.38−25.03	3.22−25.01
reflns collected	7037	7775	12 523	8369	8122	6107	6482
unique reflns	3803	4062	3352	4326	4447	4102	3049
R_{int}	0.0161	0.0417	0.0501	0.0318	0.0379	0.0275	0.0552
reflns [$I > 2\sigma(I)$]	3463	3028	2805	3651	3403	3300	2634
R1 [$I > 2\sigma(I)$] [b]	0.0210	0.0345	0.0321	0.0265	0.0465	0.0376	0.0400
wR2 (all data) [c]	0.0475	0.0725	0.0703	0.0583	0.1105	0.0850	0.0905
GOF on F^2	1.045	1.021	1.085	1.041	1.106	1.023	1.034
completeness	0.995	0.995	0.996	0.997	0.995	0.996	0.991

[a] λ (Mo Kα) = 0.71073 Å. [b] $R1 = \sum||F_o| - |F_c||/\sum|F_o|$. [c] $wR2 = [\sum w(F_o^2 - F_c^2)^2/\sum wF_o^4]^{1/2}$.

in calculated positions [C−H = 1.00 Å for C*H*$(CH_3)_2$, 0.98 Å for CH(C*H*$_3)_2$, and 0.95 Å for Phenyl hydrogens]. The isotropic thermal parameters of the hydrogen atoms were fixed at 1.2 times to that of the corresponding carbon for C*H*$(CH_3)_2$ and phenyl hydrogens, and 1.5 times for CH(C*H*$_3)_2$. In the final refinement, the hydrogen atoms were riding with the carbon atom to which they were bonded. The scattering factors for the neutral atoms were those incorporated with the programs. Crystallographic data are summarized in Table 1.

Computational Details. DFT calculations were performed primarily for compounds **3b** and **3c**. The molecular structures were optimized by using a combination of the hybrid PBE0 exchange−correlation functional[21] with the Ahlrichs' triple-ζ valence basis set augmented by one set of polarization functions (TZVP);[22] for tellurium, the corresponding ECP basis set was used. Excitation energies were calculated using the TDDFT formalism; the same density functional−basis set combination as used in the geometry optimizations was utilized. All calculations were performed with Turbomole 5.8[22] and Gaussian 03[23] program packages.

Results and Discussion

Synthesis of 6 and 7. The hexafluoroantimonate salts **6** and **7** are readily obtained in excellent yields by the reactions of **4** and **5**, respectively, with $AgSbF_6$ in a 1:1 molar ratio in toluene (eq 1).

$$[N(P^iPr_2E)_2]I + AgSbF_6 \rightarrow [N(P^iPr_2E)_2]SbF_6 + AgI \quad [E = Se\ (\mathbf{6}),\ Te\ (\mathbf{7})] \qquad (1)$$

The multinuclear NMR spectra of **6** and **7** reveal very similar features to those observed for the corresponding iodide salts **4** and **5**.[16] The $^{31}P\{^1H\}$ NMR spectra of **6** and **7** are comprised of a singlet at δ 113.2 and 85.7, respectively, with a set of ^{77}Se and ^{125}Te satellites arising from the AA′X spin system of magnetically inequivalent phosphorus atoms. Similarly to **4** and **5**, the singlets observed for both **6** and **7** do not resolve into two doublets even at low temperature (−100 °C), indicating a weak interaction of the anion with the cyclic cation that is symmetrical with respect to the chalcogen−chalcogen bond in solution.[24] This conclusion is supported by the ^{77}Se and ^{125}Te NMR spectrum of **6** and **7**, which exhibit a doublet at δ 344 [$^1J(^{77}Se,^{31}P) = 360$ Hz] and a doublet at δ 254 [$^1J(^{125}Te,^{31}P) = 870$ Hz], respectively,

(19) Sheldrick, G. M. *SHELXS-97, Program for Crystal Structure Determination*, University of Göttingen: Göttingen, Germany, 1997.
(20) Sheldrick, G. M. *SHELXL-97, Program for Crystal Structure Refinement*, University of Göttingen: Göttingen, Germany, 1997.
(21) (a) Perdew, J. P.; Burke, K.; Ernzerhof, M. *Phys. Rev. Lett.* **1996**, *77*, 3865. (b) Perdew, J. P.; Burke, K.; Ernzerhof, M. *Phys. Rev. Lett.* **1997**, *78*, 1396. (c) Perdew, J. P.; Ernzerhof, M.; Burke, K. *J. Chem. Phys.* **1996**, *105*, 9982. (d) Ernzerhof, M.; Scuseria, G. E. *J. Chem. Phys.* **1999**, *110*, 5029.
(22) All basis sets were used as they are referenced in the Turbomole 5.8 internal basis set library. Ahlrichs, R.; et al. *TURBOMOLE, Program Package for ab initio Electronic Structure Calculations, Version 5.8*; Theoretical Chemistry Group, University of Karlsruhe: Karlsruhe, Germany, 2005.
(23) Frisch, M. J.; Trucks, G. W.; Schlegel, H. B.; Scuseria, G. E.; Robb, M. A.; Cheeseman, J. R.; Montgomery, J. A., Jr.; Vreven, T.; Kudin, K. N.; Burant, J. C.; Millam, J. M.; Iyengar, S. S.; Tomasi, J.; Barone, V.; Mennucci, B.; Cossi, M.; Scalmani, G.; Rega, N.; Petersson, G. A.; Nakatsuji, H.; Hada, M.; Ehara, M.; Toyota, K.; Fukuda, R.; Hasegawa, J.; Ishida, M.; Nakajima, T.; Honda, Y.; Kitao, O.; Nakai, H.; Klene, M.; Li, X.; Knox, J. E.; Hratchian, H. P.; Cross, J. B.; Bakken, V.; Adamo, C.; Jaramillo, J.; Gomperts, R.; Stratmann, R. E.; Yazyev, O.; Austin, A. J.; Cammi, R.; Pomelli, C.; Ochterski, J. W.; Ayala, P. Y.; Morokuma, K.; Voth, G. A.; Salvador, P.; Dannenberg, J. J.; Zakrzewski, V. G.; Dapprich, S.; Daniels, A. D.; Strain, M. C.; Farkas, O.; Malick, D. K.; Rabuck, A. D.; Raghavachari, K.; Foresman, J. B.; Ortiz, J. V.; Cui, Q.; Baboul, A. G.; Clifford, S.; Cioslowski, J.; Stefanov, B. B.; Liu, G.; Liashenko, A.; Piskorz, P.; Komaromi, I.; Martin, R. L.; Fox, D. J.; Keith, T.; Al-Laham, M. A.; Peng, C. Y.; Nanayakkara, A.; Challacombe, M.; Gill, P. M. W.; Johnson, B.; Chen, W.; Wong, M. W.; Gonzalez, C.; Pople, J. A. *Gaussian 03*, revision C.02; Gaussian, Inc.: Wallingford, CT, 2004.

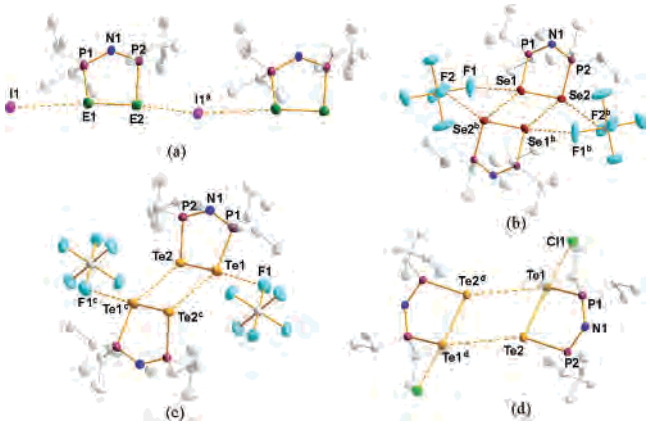

Figure 1. Molecular structures of (a) $[N(P^iPr_2Se)_2]I$ (**4**) and $[N(P^iPr_2Te)_2]I$ (**5**),[16] (b) $[N(P^iPr_2Se)_2]SbF_6$ (**6**), (c) $[N(P^iPr_2Te)_2]SbF_6$ (**7**), and (d) $[N(P^iPr_2Te)_2]Cl$ (**8**) with the atomic numbering scheme. Hydrogen atoms have been omitted for clarity. Symmetry operation: [a] $x, y-1, z$; [b] $2-x, 1-y, 1-z$; [c] $1-x, 1-y, -z$; [d] $1-x, 1-y, 1-z$.

consistent with a single chalcogen environment in each case. The ^{1}H NMR spectra of **6** and **7** display two overlapping sets of septets (appearing as an octet) for the CH hydrogens and two sets of doublets of doublets for the CH_3 hydrogens. Consistently, the $^{13}C\{^1H\}$ NMR spectra show a multiplet for the α-carbons of the $CH(CH_3)_2$ groups and two singlets for the CH_3 carbons, indicating two inequivalent isopropyl groups. Taken together, these NMR data suggest that the cationic five-membered rings in **4**−**7** retain their nonplanar structures and C_2 symmetry in solution.

The replacement of the I^- counterion by SbF_6^- results in a shift of the ^{31}P NMR resonances to higher frequency by ca. 20 ppm for both the selenium- and tellurium-containing cations, indicating decreased shielding for the phosphorus atoms in the hexafluoroantimonate salts. A shift to higher frequency is also observed for the doublet in the ^{77}Se NMR spectra of **4** and **6** (δ 297 and 344, respectively). The replacement of the I^- counterion by SbF_6^- also results in a decrease in the magnitude of the $^1J(^{77}Se,^{31}P)$ and $^1J(^{125}Te,^{31}P)$ coupling constants from 440 to 360 Hz and from 1040 to 870 Hz for the selenium- and tellurium-containing cations, respectively. At the same time, the $^2J(^{31}P,^{31}P)$ coupling constants increase slightly (by ca. 10 Hz).

Crystal Structures of 4−8. The molecular structures of **4**−**8** with the atomic numbering schemes are depicted in Figure 1, and selected bond parameters are summarized in Table 2. The compounds **4**−**8** are comprised of nonplanar, five-membered $[N(P^iPr_2E)_2]^+$ rings and counteranions, which interact primarily with one of the chalcogens. While the structures of **4** and **5** exhibit infinite chains of cations linked by chalcogen−iodine contacts (Figure 1a),[16] compounds **6**−**8** are comprised of centrosymmetric ion pairs, with chalcogen−chalcogen close contacts and chalcogen−halogen interactions (Figure 1b−d). The dimeric SbF_6^- salts **6** and **7** exhibit similar structural features (Figure 1b and c), but their crystal packing and crystal systems are distinct. As illustrated in Figure 2, the dimeric units in **6** are arranged in a linear fashion along the *c* axis whereas these units adopt a herringbone stacking pattern in the tellurium analogue **7**. These disparities are attributed to a slightly different orientation of the SbF_6^- anion; whereas **6** shows two Se···F contacts [2.982(3) and 3.329(2) Å], the tellurium system **7** exhibits only one Te···F contact [3.120(4) Å]. Interestingly, the crystals of **7** also display a significant pleochroism by having either a purple-red or a blue color depending on the orientation of the crystal (under both polarized and nonpolarized light). The color of the crystals of **6**, however, is independent of the crystal orientation. The pleochroism in **7** is tentatively attributed to the different packing arrangement of the dimeric units.

The most significant structural feature of **4** and **5** is the unusually long chalcogen−chalcogen bond [2.4839(9) and 2.8387(9) Å, respectively] [16] compared to the related six π-electron, five-membered cyclic cations in the salts $[PhCN_2Se_2][PF_6]$ [25a] and $[Se_3N_2][AsF_6]_2$ [25b] [Se−Se: 2.260(5) and 2.334(3) Å, respectively], and to the Te−Te bond length in the cation $[(Te_2SN_2)Cl]^+$, in which one of the Te atoms is three-coordinate [2.731(2) Å].[26] The Se−Se bond length is also significantly longer than the value of 2.4044(8) Å observed in the neutral heterocycle $Se_3(NAd)_2$, which is also a puckered five-membered ring.[27] DFT calculations[16] indicate that this elongation results from donation of electron density from a lone pair of the iodide counterion into the E−E σ^* orbital (LUMO) of the cation, cf. formation of triiodide I_3^- anion from an I^- ion and an I−I molecule.[28] The structural features of the chloride salt $[N(P^iPr_2Te)_2]Cl$ (**8**) are consistent with this interpretation by showing an even longer Te−Te bond [2.9026(7) Å] than that observed in **5** as a result of the stronger halide−chalcogen interaction. As indicated in Table 2, the calculated Te···Cl bond order in **8** is 0.35 while the Te···I bond order in **5** is only 0.09.[30] Consistently, the ion-separated salts **6** and **7**, which exhibit only very weak ionic interactions (the E···F bond order is ca. 0.02 for both **6** and **7**),[30] display chalcogen−chalcogen bond lengths that are typical of single bonds [Se−Se: 2.348(7) Å in **6** and Te−

(24) This type of bonding interaction is well established in the solid-state structures of halide salts of certain cationic sulfur−nitrogen ring systems, e.g., 1,2,3,4-dithiadiazolylium chlorides $[RCN_2S_2]Cl$ and $[S_4N_3]Cl$: (a) Rawson, J. R.; Banister, A. J.; Lavender, I. *Adv. Heterocycl. Chem.* **1995**, *62*, 137. (b) Galan-Mascaros, J.-R.; Slawin, A. M. Z.; Woollins, J. D.; Williams, D. J. *Polyhedron* **1996**, *15*, 4603.

(25) (a) Belluz, P. D. B.; Cordes, A. W.; Kristof, E. M.; Kristof, P. V.; Liblong, S. W.; Oakley, R. T. *J. Am. Chem. Soc.* **1989**, *111*, 9276. (b) Haas, A.; Kasprowski, J.; Pryka, M. *J. Chem. Soc., Chem. Commun.* **1992**, 1144.

(26) The Te−Te bond lengths of ditellurides are typically in the range 2.68−2.71 Å, but a value of 2.77 Å has been reported recently for the highly crowded system $(PhMe_2Si)_3CTe-TeC(SiMe_2Ph)_3$: Klapötke, T. M.; Krumm, B.; Nöth, H.; Gálvez-Ruiz, J. C.; Polborn, K.; Schwab, I.; Suter, M. *Inorg. Chem.* **2005**, 44, 5254.

(27) Maaninen, T.; Tuononen, H. M.; Schatte, G.; Suontamo, R.; Valkonen, J.; Laitinen, R.; Chivers, T. *Inorg. Chem.* **2004**, *43*, 2097.

(28) The structures of the almost linear anion $[Te_3Ph_3]^-$ (Te−Te 2.939(1) and 3.112(1) Å) and the bent cation $[Te_3Ph_3]^+$ (Te−Te 2.979(1) and 3.049(1) Å) have been compared to that of I_3^-.[29]

(29) (a) Hillier, A. C.; Liu, S.-Y.; Sella, A.; Elsegood, M. R. J. *Angew. Chem. Int. Ed.* **1999**, *38*, 2745. (b) Jeske, J.; du Mont, W.; Jones, P. G. *Angew. Chem., Int. Ed. Engl.* **1997**, *36*, 2219.

(30) The bond orders were calculated by the Pauling equation $N = 10^{(D-R)/0.71}$,[31] where R is the observed bond length (Å). The single bond length D is estimated from the sums of appropriate covalent radii (Å):[31] Te−Te 2.74, Te−I 2.70, Te−Cl 2.36, Te−F 1.95, Se−Se 2.34, Se−I 2.50, Se−F 1.77.

Table 2. Selected Bond Lengths (Å) and Bond Angles (deg) in **4**−**9** [Calculated Bond Orders in Square Brackets[30]]

	4[16]	**5**[16]	**6**	**7**	**8**	**9**
E1−E2	2.484(1) [0.63]	2.840(1) [0.72]	2.348(1) [0.97]	2.7162(7) [1.08]	2.9026(7) [0.59]	2.846(1) [0.71]
E1−P1	2.273(2)	2.396(3)	2.273(1)	2.497(2)	2.500(1)	2.510(1)
E2−P2	2.229(2)	2.437(3)	2.2628(9)	2.485(2)	2.443(1)	2.457(1)
P1−N1	1.593(5)	1.621(6)	1.595(2)	1.588(5)	1.592(4)	1.586(4)
P2−N1	1.590(5)	1.552(6)	1.591(2)	1.596(4)	1.596(4)	1.601(3)
E1···X1	3.150(1) [0.12]	3.430(1) [0.09]	2.981(3) [0.02]	3.120(4)	2.687(2) [0.35]	3.169(1) [0.22]
E1···E1′			3.868(2)[b] [0.04]			3.917(2)[e] [0.02]
E1···E2′			3.911(1)[b] [0.006]	4.0302(8)[c] [0.02]	4.3112(8)[d] [0.006]	
E2···X1′	4.006(1)[a] [0.008]	3.494(1)[a] [0.08]				3.737(1)[e] [0.03]
E2···X2′			3.329(2)[b] [0.006]			
E2···E2′					3.584(1) [0.06]	
P1−N1−P2	128.3(4)	133.2(4)	126.1(1)	130.6(3)	131.7(3)	130.3(2)
N1−P1−E1	108.4(2)	109.6(2)	106.73(9)	108.1(2)	111.2(2)	111.4(1)
N1−P2−E2	108.7(2)	109.4(2)	107.94(8)	109.5(2)	110.5(2)	112.4(1)
P1−E1−E2	91.41(4)	88.56(5)	92.60(3)	88.57(4)	86.56(3)	87.73(4)
P2−E2−E1	93.94(4)	88.36(5)	93.81(3)	89.38(4)	88.53(3)	89.95(4)
P1−E1−E2−P2	25.05(7)	25.84(7)	29.10(3)	28.15(5)	25.88(4)	21.16(3)

[a] Symmetry operation: $x, y - 1, z$. [b] $2 - x, 1 - y, 1 - z$. [c] $1 - x, 1 - y, -z$. [d] $1 - x, 1 - y, 1 - z$. [e] $1 - x, 2 - y, 1 - z$.

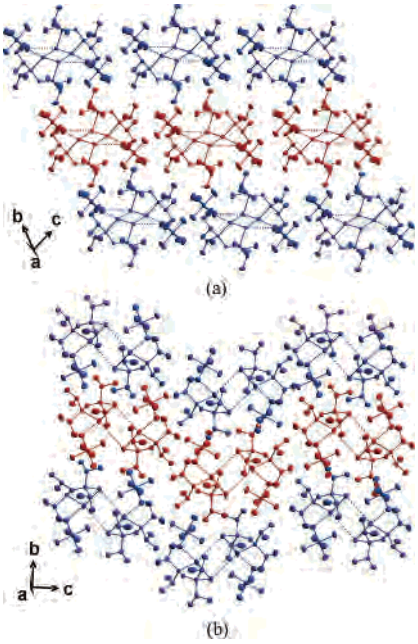

Figure 2. Crystal packing in (a) **6** and (b) **7** viewed along the *a* axis. Hydrogen atoms have been omitted for clarity.

Te: 2.7162(7) Å in **7**]. These values are also in excellent agreement with the calculated values of 2.364 and 2.726 Å for the bare cations **3b** and **3c**, respectively.

While the halide-chalcogen interactions result in a significant disparity (of 0.04−0.06 Å) in the P−E bond lengths in **4**, **5** and **8**, the corresponding distances in **6** and **7** show very small differences of ca. 0.01 Å. Changing the anion from a halide to SbF_6^- has very little effect on the average P−E and P−N bond lengths. The mean P−Se distances are 2.25 and 2.26 Å in **4** and **6**, respectively, and the P−Te bond lengths are 2.41, 2.49 and 2.47 Å in **5**, **7** and **8**, respectively. The mean P−N bond lengths in compounds **4**-**8** span the narrow range of 1.589−1.594 Å.

The average P−N−E bond angles in **4**−**8** are close to the ideal tetrahedral values, varying from 107.3° in **6** to 110.9° in **8**. A P1−E1−E2−P2 dihedral angle of ca. 25.6° is observed for the halide salts **4**, **5**, and **8**, while the SbF_6^- salts show a slightly larger value of ca. 28.6°. The P−E−E bond angles are more dependent on the strength of the anion interaction to one of the two chalcogens. Thus, **4** and **8** show a difference of ca. 2.5° and 2.0° between the P1−E1−E2 and P2−E2−E1 angles, respectively, whereas the corresponding difference in the SbF_6^- salts **6** and **7** is only ca. 1°. The P−E−E angles in **5** are equal within experimental error due to the two almost identical Te···I close contacts in the solid state [Te1···I1: 3.430(1) Å and Te2···I1[a]: 3.494(1) Å]. Expectedly, the elongation of the chalcogen−chalcogen bond has a noticeable effect on the P−N−P angles, which are somewhat wider in the halide salts **4**, **5**, and **8** than in the hexafluoroantimonate salts **6** and **7**.

In the Raman spectrum of **4**, the most intense band at 195 cm^{-1} is attributed to the Se−Se stretching vibration, which is shifted to 255 cm^{-1} in **6** reflecting the decrease in the Se−Se bond length. Both of these Raman lines correlate well with, for example, the ν(Se−Se) stretching vibration at 269 cm^{-1} observed for $[(Se_2SN_2)Cl]_2$, which exhibits a Se−Se bond length of 2.3464(7) Å.[32] The Te−Te stretching vibrations show similar behavior; the most intense Raman line at 149 cm^{-1} observed for **5** shifts to 165 cm^{-1} for **7**. The latter value can be compared to the band at 167 cm^{-1} observed for diphenyl ditelluride $(PhTe)_2$[33] which has a Te−Te bond length of 2.712(2) Å.[34]

UV−Visible Spectra. The assignments of the absorptions observed in the UV−visible spectra of compounds **4**−**7** were guided by the TDDFT excitation energy calculations carried out for the bare cations **3b** and **3c**. The selenium-containing **4** and **6** exhibit broad absorptions in the region 230−270 and at 365 nm in CH_2Cl_2, as well as a "tail" with a significantly lower molar absorptivity at ca. 450 nm as expected from the yellow-orange color of solutions. The

(31) Pauling, L. *The Nature of the Chemical Bond*, 3rd ed.; Cornell University Press: Ithaca, NY, 1960.
(32) Maaninen, A.; Konu, J.; Laitinen, R. S.; Chivers, T.; Schatte, G.; Pietikäinen, J.; Ahlgrén, M. *Inorg. Chem.* **2001**, *40*, 3559.
(33) McWhinnie, W. R.; Thavornyutikarn, P. J. *Organomet. Chem.* **1972**, *35*, 149.
(34) Llabres, P. G.; Dideberg, O.; Dupont, L. *Acta Crystallogr.* **1972**, *B28*, 2438.

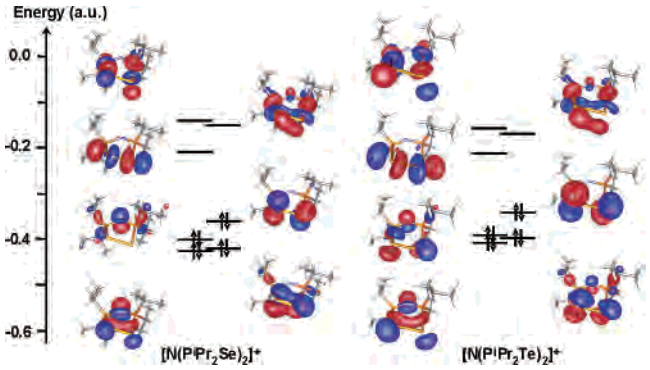

Figure 3. Frontier molecular orbitals and energy levels in the $[N(P^iPr_2E)_2]^+$ rings (E = Se, Te).

absorption in the visible region is attributed to the HOMO→LUMO transition ($\pi^*\rightarrow\sigma^*$, Figure 3) and is computationally predicted to appear at 460 nm. The calculations for **3b** also show several transitions in the 230−270 nm region; those with the highest oscillator strength correspond to the HOMO-4→LUMO ($\sigma\rightarrow\sigma^*$), HOMO→LUMO+2 ($\pi^*\rightarrow\sigma^*$) and HOMO-1→LUMO+1 ($\pi^{NB}\rightarrow\sigma^*$) transitions.

The tellurium-containing compounds **5** and **7** exhibit broad absorptions at ca. 230−270 and 365 nm, and **7** also shows a weak absorption at 560 nm in MeCN that shifts to 595 nm in CH_2Cl_2, reflecting the different colors of these solutions (purple-red in MeCN and greenish-blue in CH_2Cl_2). Like the selenium compounds **4** and **6**, the visible absorption band is attributed to the HOMO→LUMO transition ($\pi^*\rightarrow\sigma^*$, Figure 3) and is computationally predicted to occur at 554 nm. The most significant transitions in the 230−270 nm region are HOMO-2→LUMO+1 ($\pi\rightarrow\sigma^*$), HOMO→LUMO+2 ($\pi^*\rightarrow\sigma^*$), and HOMO-1→LUMO+2 ($\pi^{NB}\rightarrow\sigma^*$).

Surprisingly, the calculations predict no excitations at ca. 365 nm, although bands in this region with high molar absorptivities are observed experimentally. In compounds **4**−**7**, these absorptions are tentatively attributed to cation−anion interactions, which were not included in the calculations. This hypothesis is supported by the observation that the molar absorptivity for the 365 nm band decreases by an order of 10 when the counterion is changed from I^- to SbF_6^-. Furthermore, TDDFT calculations for **5,** with variation of the Se···I distances, reveal the appearance of new transitions in the 320−380 nm range. As expected, these transitions have relatively high predicted oscillator strengths and involve excitations from the inner occupied MOs centered mostly on the halogen atom to the Se−Se−I antibonding LUMO of the complex. The inclusion of a counterion also has an influence on the calculated HOMO→LUMO transitions. Although the excitation energy remains essentially unchanged at 460 ± 10 nm, a significant decrease in the oscillator strength is predicted. These findings are consistent with the observation that transitions in the visible region of the spectrum are only observed for compounds **5** and **7** and not for **4** and **6**.

Synthesis and Structure of 9. The reaction between the phenyl-substituted $[(TMEDA)NaN(PPh_2Te)_2]$ and I_2 produces **9** as a red-brown powder. However, the yield of **9** is 66%,

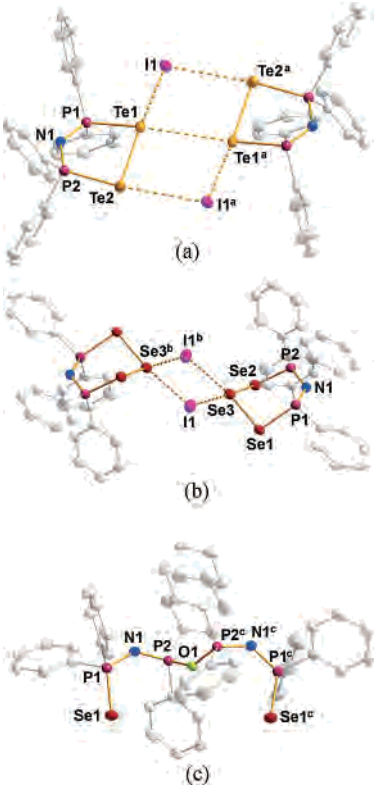

Figure 4. Molecular structures of (a) $[N(PPh_2Te)_2]I$ (**9**), (b) $[N(PPh_2Se)_2(\mu\text{-Se})][I]$ (**10**), and (c) $\{[N(PPh_2)_2Se]_2(\mu\text{-O})\}\cdot CH_2Cl_2$ (**12**·CH_2Cl_2) with the atomic numbering scheme. Hydrogen atoms and the solvent molecule in the structure **12**·CH_2Cl_2 have been omitted for clarity. Symmetry operation: [a] $1-x, 2-y, 1-z$; [b] $1-x, 1-y, -z$; [c] $1-x, y, 1.5-z$.

significantly lower than the 92% yield achieved for the isopropyl analogue **5**.[16] Complex **9** was characterized by multinuclear NMR spectra and, after recrystallization from CH_2Cl_2, by a single-crystal X-ray structural determination. The $^{31}P\{^1H\}$ NMR spectrum of **9** in CH_2Cl_2 consists of a singlet at 21.9 ppm with ^{125}Te satellites ($^1J(^{125}Te,^{31}P) = 1066$ Hz, cf. 1040 Hz for **5**). In contrast to the isopropyl derivatives **4**−**7**, the two bond $^{31}P-^{31}P$ coupling is not resolved for **9**, owing to the significantly broader signals. The ^{125}Te NMR signal could not be observed because of the low solubility of **9**.

The structural features of the five-membered cyclic cation in **9** (Figure 4a) resemble those of the isopropyl derivative **5**. Selected bond parameters are given in Table 2. In contrast to **5**, however, the phenyl derivative **9** exists as a centrosymmetric ion pair with a significantly shorter Te···I close contact than that observed in **5** (3.169(1) Å in **9** vs 3.430(1) Å in **5**). Despite the stronger Te···I interaction, the Te−Te bond lengths in **9** and **5** of 2.846(1) and 2.840(1) Å, respectively, are indistinguishable. The P−Te bonds in **9** are ca. 0.07 Å longer than those observed in **5** but are close to the corresponding bond lengths in the chloride salt **8**. In addition, the five-membered rings in **5** and **8** are slightly more puckered than that in **9**, as reflected in the larger (by ca. 4.7°) P1−Te1−Te2−P2 dihedral angle.

Reaction of $[(TMEDA)NaN(PPh_2Se)_2]$ with I_2. In contrast to the successful preparation of the tellurium-containing compound **9**, the attempted synthesis of the selenium

Table 3. Selected Bond Lengths (Å) and Bond Angles (deg) in **10**, **12**·CH_2Cl_2, and **13**

		10	
Se1−Se3	2.441(1)	P1−N1	1.588(6)
Se2−Se3	2.427(1)	P2−N1	1.591(6)
Se1−P1	2.222(2)	Se3···I1	3.102(1)
Se2−P2	2.202(2)	Se3···I1′	3.140(1)[a]
P1−N1−P2	131.7(4)	P1−Se1−Se2	98.14(6)
N1−P1−Se1	115.7(2)	P2−Se2−Se3	96.38(6)
N1−P2−Se2	116.0(2)	Se1−Se2−Se3	95.64(4)
		12·CH_2Cl_2	
Se1−P1	2.117(1)	P2−N1	1.549(3)
P1−N1	1.620(3)	O1−P2	1.619(1)
Se1−P1−N1	118.4(1)	P2−O1−P2′	139.8(2)[b]
P1−N1−P2	135.6(2)	P1−N1−P2−O1	63.3(3)
N1−P2−O1	115.3(1)	P2−N1−P1−Se1	8.7(3)
		13	
Se1−P1	2.125(1)	P1−N1	1.626(3)
Cl1−P2	2.050(2)	P2−N1	1.532(3)
Se1−P1−N1	118.1(1)	P1−N1−P2−Cl1	43.5(5)
P1−N1−P2	147.0(2)	P2−N1−P1−Se1	8.3(6)
N1−P2−Cl1	114.9(1)		

[a] Symmetry operation: $1 - x, 1 - y, -z$. [b] $1 - x, y, 1.5 - z$.

analogue, $[N(PPh_2Se)_2]I$, by the reaction of $[(TMEDA)NaN(PPh_2Se)_2]$ and I_2 in a 1:1 molar ratio afforded an equimolar mixture of **10** and **11** (Scheme 1).

The identity of **10** was determined by an X-ray structural determination. The molecular structure with the atomic numbering scheme is depicted in Figure 4b, and the relevant bond parameters are summarized in Table 3. The structure of **10** consists of a centrosymmetric dimer formed by two cyclic six-membered cations in a chair conformation and two bridging I^- anions.[35] The Se3 atom exhibits two similar Se···I close contacts [Se3···I1 3.102(1) Å and Se3···I1[b] 3.140(1) Å] and two almost equal Se−Se bond lengths [Se1−Se3 2.441(1) Å and Se2−Se3 2.427(1) Å], resulting in a slightly distorted square plane. The mean Se−Se distances are ca. 0.21 Å shorter than those observed in the square-planar complex $\{[N(P^iPr_2Se)_2]_2(\mu\text{-Se})\}$,[37] which can be described as consisting of two $[N(P^iPr_2Se)_2]^-$ anions chelated to a central Se^{2+} cation.[37] The stronger interaction of a single $[N(P^iPr_2Se)_2]^-$ anion with a Se^{2+} cation may explain the shorter Se−Se bond lengths in **10**. The Se−Se bond lengths and Se···I close contacts in the dimer **10** are comparable to those observed in the iodide salt of the five-membered cyclic cation **4**. The Se−P and P−N bond lengths are also similar to those found in the five-membered rings **4** and **6**. The more open Se1−P1−N1−P2−Se2 unit in **10** compared to the closed cyclic structure in **4** and **6** is reflected in both the P−N−P and N−P−Se bond angles, which are ca. 5° and 8° wider in **10** than in **4** and **6**, respectively. The crystal packing in **10** results in planar arrangement of two of the phenyl groups with the nitrogen atom located between the rings (Figure 5).

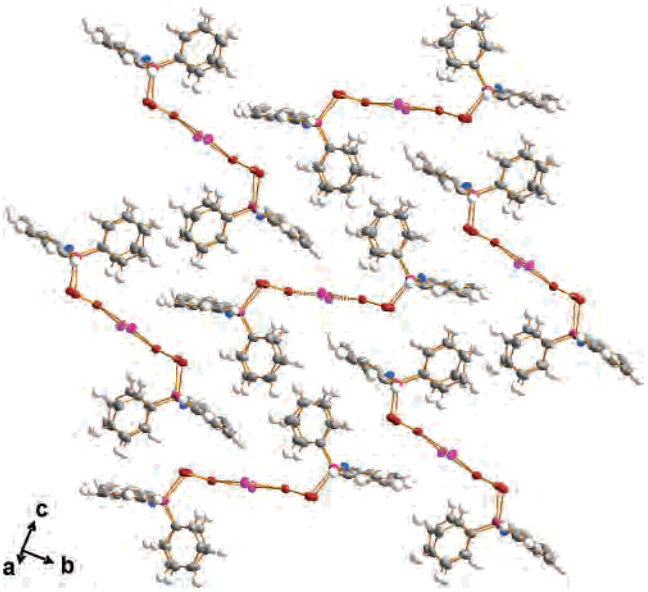

Figure 5. Crystal packing in **10** showing the planar arrangement of the phenyl groups.

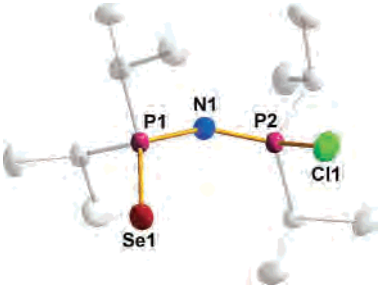

Figure 6. Molecular structure of $[SeP(^iPr_2)N(^iPr_2)PCl]$ (**13**). Hydrogen atoms have been omitted for clarity.

The identity of the second product **11** was established by an X-ray structural determination of the hydrolysis product **12**·CH_2Cl_2 and is supported by the ^{31}P NMR data (see discussion below). The crystal structure determination of **12**·CH_2Cl_2[38] (Figure 4c) revealed a nine-atom Se−P−N−P−O−P−N−P−Se chain with selenium atoms in a cis configuration. Selected bond parameters for **12**·CH_2Cl_2 are given in Table 3. The Se−P bond length [2.117(1) Å] is comparable to the value of 2.120(2) Å observed for the terminal P═Se bonds in the eight-atom chain $[Se{=}P(Ph_2)N(Ph_2)P-P(Ph_2)N(Ph_2)P{=}Se]$.[40] The significant difference between the P1−N1 [1.620(3) Å] and P2−N1 [1.549(3) Å] bond lengths is consistent with the bonding arrangement for **12** depicted in Scheme 1.

Formation of 10 and 12. The reaction of $[(TMEDA)NaN(PPh_2Se)_2]$ and I_2 in a 1:1 molar ratio was repeated several times, and the $^{31}P\{^1H\}$ NMR spectrum of the product mixture was comprised consistently of three singlets at δ 49.5, 36.1, and 24.3 with an intensity ratio of 2:1:1. The broad resonance at δ 49.5 shows ^{77}Se satellites. The

(35) The structure of an analogous six-membered ring system in the dimer $[N(PPh_2S)_2Te(\mu\text{-Cl})]_2$ has been reported.[36]
(36) Novosad, J.; Törnroos, K. W.; Necas, M., Slawin, A. M. Z., Woollins, J. D.; Husebye, S. *Polyhedron* **1999**, *18*, 2861.
(37) Cea-Olivares, R.; Moya-Cabrera, M.; Garcia-Montalvo, V.; Castro-Blanco, R.; Toscano, R. A.; Hernandez-Ortega, S. *Dalton Trans.* **2005**, 1017.
(38) The structure of **12,** obtained as a hydrolysis product of $K[N(PPh_2Se)_2]$, has been mentioned briefly in a review,[39] but details of the crystallographic and structural data have not been reported.
(39) Woollins, J. D. *J. Chem. Soc., Dalton Trans.* **1996**, 2893.
(40) Slawin, A. M. Z.; Smith, M. B.; Woollins, J. D. *Chem. Commun.* **1996**, 2095.

Scheme 1

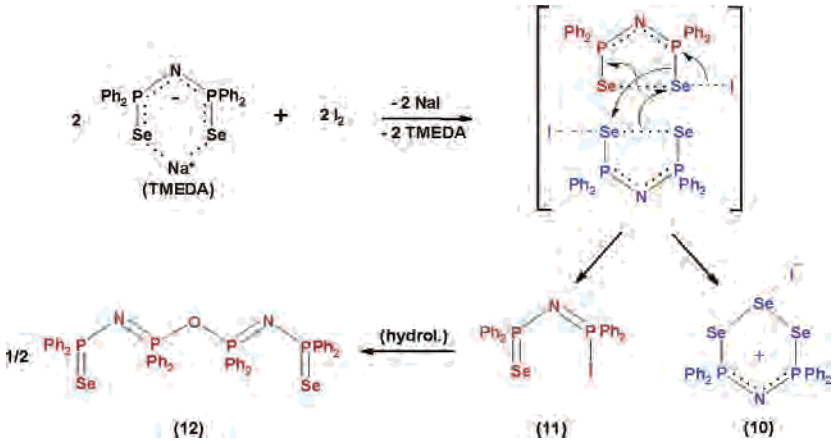

magnitude of the coupling constant $^1J(^{31}P,^{77}Se) = 447$ Hz implies a P−Se bond order of about 1,[41] and hence, this resonance is attributed to the cyclic cation in **10**. Although the two singlets at δ 36.1 and 24.3 do not exhibit $^{31}P-^{31}P$ coupling, these resonances consistently appeared with 1:1 relative intensities, and therefore, they are assumed to arise from a single compound. The former resonance exhibits ^{77}Se satellites with $^1J(^{31}P,^{77}Se) = 745$ Hz, which is consistent with a terminal P═Se bond,[41] while the latter resonance exhibits no ^{77}Se satellites. In light of these NMR data, we tentatively suggest that **11** is the acyclic compound [SeP(Ph_2)N(Ph_2)-PI]. As indicated in Scheme 1, the hydrolysis of this species during recrystallization gives rise to the structurally characterized nine-atom chain **12**.[42,43]

To explain the formation of equimolar amounts of **10** and **11** in the reaction of [(TMEDA)NaN($PPh_2Se)_2$] and I_2, we propose the initial formation of the five-membered ring, $[N(PPh_2Se)_2]^+$, and subsequent decomposition of this cyclic cation by an intermolecular process (Scheme 1). To provide some insight into the occurrence of this decomposition process for $[N(PPh_2Se)_2]^+$, but not for the tellurium analogue $[N(PPh_2Te)_2]^+$, DFT calculations of the formation energies of a 1:1 mixture of the two products $[N(PR_2E)_2(\mu\text{-}E)][I]$ and [EP(R_2)N(R_2)PI] (E = Se, Te; R = H, ^{i}Pr, Ph) were carried out. The conversion of two molecules of $[N(PPh_2Se)_2]I$ into **10** and **11** was found to be approximately thermoneutral in the gas phase, whereas the analogous process for **4**, **5**, and **9** is endothermic by ca. 55, 85, and 50 kJ mol^{-1}, respectively; the calculated reaction energies for the hypothetical R = H structures were highly endothermic (>100 kJ mol^{-1}). Although these calculations do not consider the kinetic aspects of the reaction or the relative lattice energies of salts containing the five- or six-membered cyclic cations, the trend in formation energies is nevertheless consistent with the experimentally observed decomposition of $[N(PPh_2Se)_2]I$. It is conceivable that the instability of the five-membered ring in this case results from an enhancement of the $I^-\rightarrow$Se−Se-(σ^*) electron transfer caused by the electron-withdrawing phenyl substituents on phosphorus and a concomitant weakening of the Se−Se bond.

Formation and Structure of [SeP(^{i}Pr$_2$)N(^{i}Pr$_2$)PCl] (13). The reaction of [(TMEDA)NaN($P^iPr_2Se)_2$] with $SeCl_2$ was carried out in a 1:1 molar ratio in an attempt to generate the isopropyl derivative of the six-membered ring in **10** as the chloride salt. However, instead of the expected product, the acyclic compound **13** was obtained in 39% yield (eq 2). This unsymmetrical derivative was characterized by multinuclear NMR spectra and by an X-ray structural determination.[44]

$$[(\text{TMEDA})\text{NaN}(P^iPr_2Se)_2] + SeCl_2 \rightarrow [\text{SeP}(^iPr_2)\text{N}(^iPr_2)\text{PCl}] + \text{NaCl} + \text{TMEDA} + 1/4Se_8 \quad (2)$$

The $^{31}P\{^1H\}$ NMR spectrum of **13** is comprised of two mutually coupled doublets at δ 67.2 and 66.0 with $^2J(^{31}P,^{31}P) = 37$ Hz. The former resonance shows ^{77}Se satellites with $^1J(^{77}Se,^{31}P) = 722$ Hz, cf. 745 Hz in **11**, consistent with a terminal P═Se bond.[41] The $^{77}Se\{^1H\}$ NMR spectrum of **13** exhibits a doublet at δ −308 with $^1J(^{77}Se,^{31}P) = 722$ Hz. As expected for this unsymmetrical derivative, the $^{13}C\{^1H\}$ and ^1H NMR spectra exhibit resonances that are more widely separated than those observed for **4**−**8**, owing to the significant difference in the environments of the isopropyl groups in **13**.

The molecular structure of **13** (Figure 6) shows a cis arrangement for the terminal selenium and chlorine atoms of the distorted SePNPCl chain similar to the configuration

(41) Briand, G. G.; Chivers, T.; Krahn, M.; Parvez, M. *Inorg. Chem.* **2002**, *41*, 6808 and references therein.

(42) The hydrolysis product {[N($PPh_2)_2Se]_2(\mu$-O)} (**12**) is also expected to give rise to two resonances with a relative intensity of 1:1, one of which would show a $^1J(^{77}Se,^{31}P)$ coupling constant in the region 720−750 Hz for the terminal P═Se bond. It is highly unlikely, however, that the solvent used in several different reactions would contain the exact amount of water to give a 2:1 mixture of **10** and the hydrolysis product **12** that is required to generate three resonances with a 2:1:1 intensity ratio in the ^{31}P NMR spectrum (see Scheme 1).[43]

(43) The reaction between [(TMEDA)NaN($PPh_2Se)_2$] and I_2 was also conducted in *n*-hexane/toluene solution and gave a 1:1 mixture of **10** and **11** (^{31}P NMR spectrum), thus precluding the unlikely possibility that THF is the source of oxygen in the formation of **12**.

(44) The syntheses of the following related acyclic compounds EP(R_2)-NP(R_2)X (E = chalcogen; X = halogen) have been reported without structural characterization: [SP(Ph_2)N(Ph_2)PCl],[45a] [SP(Ph_2)N(Ph_2)-PCl]HCl,[45a] [SP(Ph_2)N(Ph_2)PBr],[45b] [OP(Ph_2)N(Ph_2)PCl],[45c] and [OP-(Ph_2)N(Ph_2)PBr]Br.[45d]

(45) (a) Schmidpeter, A.; Groeger, H. *Chem. Ber.* **1967**, *100*, 3979. (b) Meinel, L.; Nöth, H. *Z. Anorg. Allg. Chem.* **1970**, *373*, 36. (c) Gilson, I. T.; Sisler, H. H. *Inorg. Chem.* **1965**, *4*, 273. (d) Baldwin, R. A.; Washburn, R. M. *J. Org. Chem.* **1965**, *30*, 2093.

of the selenium atoms in the symmetrical derivative [SeP(^{i}Pr$_2$)NH(^{i}Pr$_2$)PSe].[7] Selected bond parameters for **13** are summarized in Table 3. The Se═P bond length [2.125(1) Å] is comparable to the values of 2.117(1), ca. 2.10, and 2.120(2) Å found in **12**, [SeP(^{i}Pr$_2$)NH(^{i}Pr$_2$)PSe],[7] and [Se═P(Ph$_2$)N(Ph$_2$)P−P(Ph$_2$)N(Ph$_2$)P═Se],[40] respectively. The difference between the P1−N1 and P2−N1 bond lengths of ca. 0.1 Å is comparable to that observed in **12** and suggests a trend toward single and double bond character for the two P−N bonds, respectively. The P−N−P bond angle in **13** (147.0(2)°) is substantially wider than the values of 135.6(2)°, 131.2(2)°, and 135.5(4)° observed in **12**, [SeP(^{i}Pr$_2$)NH(^{i}Pr$_2$)PSe],[7] and [Se═P(Ph$_2$)N(Ph$_2$)P−P(Ph$_2$)N(Ph$_2$)P═Se], respectively.[40] Although the P−N−P−Se dihedral angles in **12** and **13** are identical, **13** shows a less puckered chain than that of **12** [τ P−N−P−Cl in **13** is 43.5(5)°, and τ P−N−P−O in **12** is 63.3(3)°]. In the crystal lattice (see Figure S2 in the Supporting Information), **13** forms molecular strands connected by Cl···H close contacts [2.883(1) Å] that are slightly shorter than the sum of van der Waals radii (2.95 Å).[31]

Conclusions

The synthesis and structural characterization of the SbF_6^- salts of the cyclic cations $[N(P^iPr_2E)_2]^+$ (E = Se, Te) has provided experimental verification for the earlier suggestion, based on DFT calculations,[16] that the unusually long chalcogen−chalcogen bonds observed in the corresponding iodide salts can be attributed primarily to the donation of electron density from an electron pair of the halide anion into the E−E σ^* orbital (LUMO) of the ring system. Changing the substituent on phosphorus from isopropyl to the electron-withdrawing phenyl has an unanticipated influence on the outcome of the oxidation of the $[N(PR_2E)_2]^-$ anion (E = Se, Te). The tellurium-containing cation, $[N(PPh_2Te)_2]^+$, was obtained as the iodide salt, albeit in significantly lower yield than the analogous isopropyl derivative. By contrast, the attempted synthesis of the selenium analogue $[N(PPh_2Se)_2]^+$ produced a 1:1 mixture of a novel six-membered ring, $[N(PPh_2Se)_2(\mu\text{-Se})][I]$, and an acyclic species [SeP(Ph$_2$)N(Ph$_2$)PI]. DFT calculations support the suggestion that these products are formed by the decomposition of the initially formed five-membered ring $[N(PPh_2Se)_2]^+$ cation. The reaction of [(TMEDA)NaN(P^{i}Pr$_2$Se)$_2$] with $SeCl_2$ unexpectedly afforded, as the main product, the acyclic compound [SeP(^{i}Pr$_2$)N(^{i}Pr$_2$)PCl], a potentially useful reagent for the construction of chains or macrocycles in view of the reactive P−Cl functionality.

Acknowledgment. The authors gratefully acknowledge financial support from the Academy of Finland (J.K. and H.M.T.) and the Natural Sciences and Engineering Research Council (Canada). We are also thankful for Professor Michael Gerken (University of Lethbridge) for obtaining the Raman spectra.

Supporting Information Available: X-ray crystallographic files in CIF format, vibrational data (IR and Raman) for compounds **4**−**7**, **9**, and **13** (Table S1), and a figure of the extended structure of **13** in crystal lattice showing the Cl1···H22C[a] close contacts (Figure S2). This material is available free of charge via the Internet at http://pubs.acs.org.

IC061545I